Surface Engineering

ISSN: 0267-0844 (Print) 1743-2944 (Online) Journal homepage: https://www.tandfonline.com/loi/ysue20

Surface modification by multilayered Zn–Co alloy coatings

S Yogesha, K R Udupa & A C Hegde

To cite this article: S Yogesha, K R Udupa & A C Hegde (2012) Surface modification by multilayered Zn–Co alloy coatings, Surface Engineering, 28:1, 49-56, DOI: 10.1179/1743294411Y.0000000009

To link to this article: https://doi.org/10.1179/1743294411Y.0000000009

Surface modification by multilayered Zn–Co alloy coatings

S. Yogesha[1], K. R. Udupa[2] and A. C. Hegde*[1]

Nanostructured multilayer alloy or composition modulated multilayer alloy coatings of Zn–Co have been developed, and their corrosion behaviours were studied by potentiodynamic polarisation and electrochemical impedance spectroscopy methods. The coatings were developed galvanostatically using square, triangular and sawtooth current pulses through single bath technique. The cyclic cathode current density and the numbers of layers have been optimised for peak performance of the coatings against corrosion. Under optimal conditions, the coatings developed using square, triangular and sawtooth current pulses were found to be respectively ~100, 80 and 90 times more corrosion resistant than monolithic alloy of same thickness. The better corrosion resistances of the composition modulated multilayer alloy coatings were attributed to the dielectric barrier at the interface, as evidenced by dielectric spectroscopy. Surface morphology, multilayer formation and surface after corrosion tests were examined by scanning electron microscopy.

Keywords: Composition modulated multilayer alloy, Zn–Co, Square pulse, Triangular pulse, Sawtooth pulse, Corrosion resistance

Introduction

The properties of micro-/nanostructured materials basically depend on their atomic structure, composition, defects and interfaces. They are often characterised by a physical dimension of <100 nm and find applications in several domains. Composition modulated multilayer alloys (CMMAs) are one class of such micro-/nanostructured materials.[1] The CMMA coatings basically consist of ultrathin layers of different metals/alloys having thickness of a few micro-/nanometres, arranged in an alternate fashion.[2–4] As a result of layering at near atomic dimension, the nanostructured multilayered deposits can possess remarkable and sometimes unique properties not attainable in normal metallurgical alloys. These properties include X-ray optical properties, magneto-optical properties, improved hardness and wear and corrosion resistance.[5–8]

There are different methods for producing CMMA coatings, e.g. physical vapour deposition,[9–11] chemical vapour deposition[12] and electrodeposition.[13] Electrolytically, such alloys can be obtained by either single bath technique (SBT), where deposition takes place in a plating solution containing ions of the alloy components, or double bath technique, where deposition is carried out from separate plating baths using a manual and automated transfer of the substrate from one bath to another. Although gradations in composition of the deposit are possible through modulation in cathode current density (CD), agitation, temperature, etc., it can be better controlled through the cathode current/voltage, with great degree of accuracy and reproducibility, using microprocessor controlled power sources.[14–16] This technique, in principle, is straightforward to design and fabricate. The development of CMMA coatings of Zn–Fe group metals (Fe, Co, Ni and Mn) has already been reported, with evidence of its enhanced corrosion resistances.[17–20] Kalantary *et al.*[21] obtained zinc–nickel CMMA coatings with an overall thickness of 8 μm by electrodepositing alternate layers of zinc and nickel from zinc sulphate electrolyte and nickel sulphate electrolyte. Chawa *et al.*[22] reported the corrosion resistance of zinc–nickel CMMA coatings electrodeposited from zinc sulphate and nickel sulphamate baths. The corrosion resistance of zinc–nickel CMMA coatings was found to be better than that of zinc or nickel monolithic coatings of the same thickness. Zn and Zn–Ni CMMA coatings were electrodeposited on a steel substrate by the successive deposition of Zn and Zn–Ni alloy layers from dual baths.[23] Varieties of Zn and Zn–Co alloy CMMA coatings were electrodeposited onto steel substrates using the dual bath technique.[24] The experimental results showed that the Zn and Zn–Co alloy CMMA coatings are more corrosion resistant than corresponding monolithic coatings of the same thickness. The application of zinc and zinc alloy based systems was reviewed by Wilcox.[25] The concept of production of CMMA coatings, concentrating on their application as protective coatings for metal surfaces was examined. Zn–Ni, Zn–Fe, Zn–Co and Zn–Mn alloys electrodeposited in multilayer format have been reported. Deposition

[1]Electrochemistry Research Laboratory, Department of Chemistry, National Institute of Technology Karnataka, Surathkal, Srinivasnagar 575 025, India
[2]Department of Metallurgical and Materials Engineering, National Institute of Technology Karnataka, Surathkal, Srinivasnagar 575 025, India

*Corresponding author, email achegde@rediffmail.com

Published by Maney on behalf of the Institute
Received 16 July 2010; accepted 26 January 2011
DOI 10.1179/1743294411Y.0000000009

methods, bath chemistry and coating morphologies and performances in various corrosion tests were also reviewed.

Most of the work reported above explains the development of CMMA Zn based alloys using the double bath technique, in which successive layers of alternate composition were obtained from two separate electrolytes having either pure Zn^{2+} and M^{2+} (where M=Ni, Co and Fe) ions or Zn^{2+} and ($Zn^{2+}+M^{2+}$) ions. The deposition conditions were optimised, and the results were discussed. The coating behaviours were assessed either by their dissolution potentials or by E_{corr} values without determining their corrosion rates. Recently, the optimisation of an acid chloride bath for the production of CMMA Zn–Co alloy showing peak performance against corrosion using SBT was reported by Thangaraj *et al.*[26] The CMMA coatings were developed from a chloride bath having glycine as additive using square current pulses. No work is reported with regard to the development of corrosion resistant CMMA coatings using triangular and sawtooth current pulses.

In this direction, the present paper reports the development of CMMA Zn–Co coatings using different current pulses, namely, square, triangular and sawtooth (or trapezoidal), and their corrosion performance in comparison with that of monolithic alloy deposited for the same length of time. The bath constituents and the operating parameters were optimised for bright monolithic Zn–Co alloy on mild steel using thiamine hydrochloride as additive. The effects of different current pulses on deposit characters, and consequently on corrosion behaviours, were tested. The improved corrosion resistances of CMMA coatings are attributed to the changed dielectrics of the electrical double layer capacitor at the interface.

Experimental

The initial studies were focused on the optimisation of an electrolytic bath through standard Hull cell method.[27] The plating solutions were freshly prepared from distilled water and analytical grade reagents. Deposition was carried out at different current densities using optimised bath, consisting of 10 g L^{-1} ZnO, 30 g L^{-1} $CoCl_2.6H_2O$, 200 g L^{-1} NH_4Cl, 20 g L^{-1} H_3BO_3, 10 g L^{-1} $C_6H_8O_7$. H_2O and 3 g L^{-1} $C_{12}H_{17}N_4OSCl.HCl$ (thiamine hydrochloride). Electroplating of mild steel plates was carried out at pH 3·5±0·05 and temperature of 30±2°C. The polished mild steel plates (0·063C–0·23Mn–0·03S–0·011P–99·6Fe) that had exposed surface area of 7·5 cm^2 served as cathode. The anode was pure Zn with the same exposed area. A rectangular polyvinyl chloride cell containing 250 cm^3 electrolyte was used. All the depositions were carried out at a constant condition of stirring without purging to maintain a steady state of mass transport. All the coatings, namely, monolithic and CMMA, were carried out galvanostatically using a sensitive power source (N6705A, Agilent Technologies) for 10 min (~20 μm thickness) for comparison purpose.

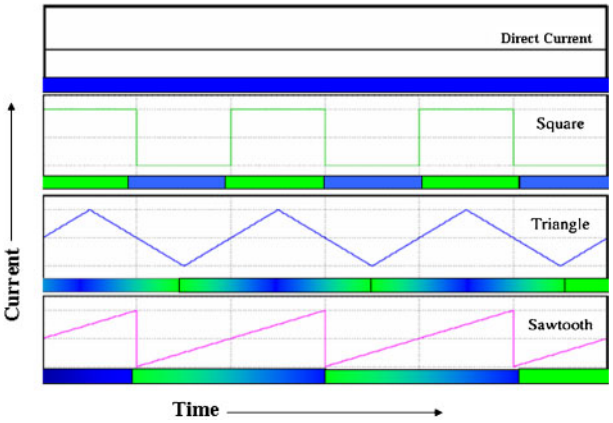

1 Schematic representation of different power patterns used and corresponding modulation in composition of alloy

The change in CD allows the growth of layers with change in chemical compositions; that is, CMMA coatings with sharp and gradual change in the Co content of alloy in alternate layers were developed using square, triangular and sawtooth current pulses. Different power patterns were used, and the corresponding modulation in composition is shown schematically in Fig. 1. The instrument was set to produce two different cathode current densities called cyclic cathode current densities (CCCDs) in a repetitive way. The thickness of each layer was controlled by the duration of each current pulse, and the total number of layers was fixed by adjusting the time for each cycle. Thus, CMMA coatings of different configurations were produced. Such multilayer coatings are hereafter represented as $(Zn–Co)_{1/2/n}$, where (Zn–Co) represents alloy of Zn and Co, 1 and 2 represent cathode CD that cycles and '*n*' represents the number of layers formed in total time (10 min).

While the thickness of the coating was estimated by Faraday's law, it was verified by measurements using a digital thickness meter (Coatmeasure model M&C). While the composition of the coatings was determined by stripping a known amount of deposit into dilute HCl solutions followed by colorimetric analysis,[28] it was verified by energy dispersive X-ray method. All the electrochemical studies were made using a potentiostat/galvanostat (VersaSTAT,[3] Princeton Applied Research)

Table 1 Composition, thickness, hardness and corrosion data of Zn–Co alloy coatings under different conditions of CD

CD/A dm^{-2}	wt-%Co	Thickness /μm	Vickers hardness /HV(100 g)	$-E_{corr}$ (Ag,AgCl/KCl_{sat})/V	i_{corr} /μA cm^{-2}	CR/$\times10^{-2}$ mm y^{-1}	Nature of the deposit
1. 0	17·0	6·2	138	1·12	20·33	30·16	Blackish
2. 0	1·77	6·8	151	1·18	13·63	20·22	Bright
3. 0	1·69	11·1	154	1·15	13·15	19·51	Bright
4·0	2·10	12·1	168	1·10	14·98	22·22	Bright
5·0	2·21	14·9	179	1·05	16·49	24·47	Bright
6·0	2·24	16·3	195	1·04	18·47	27·41	Semi bright
7·0	1·93	17·0	201	1·05	20·84	30·52	Semi bright

in a three-electrode configuration cell containing Ag/AgCl/KCl_{sat} as reference electrode. The 5% (mass per volume) NaCl solution was used as corrosion medium. The potentiodynamic polarisation study was carried out in a ramped potential of ± 250 mV, around an open circuit potential, at a scan rate of 1 mV s^{-1}. The electrochemical impedance spectroscopy (EIS) study was carried out using a perturbing signal of 10 mV in the frequency range from 100 kHz to 10 mHz. The experimental impedance data were fitted to an appropriate equivalent circuit using Zsimp Win software. The surface morphology, the multilayer formation and the possible dissolution of successive layers during corrosion were examined by scanning electron microscopy (SEM, JSM-6380 LA from JEOL, Japan).

Results and discussion

Development of monolithic Zn–Co alloy coating

Coatings of varying appearances were obtained over a wide range of current densities, i.e. 1·0–7·0 A dm^{-2}, and their corrosion data are reported in Table 1. It may be observed that the weight percentage of Co in the deposit increases as the CD increased, which is a characteristic of the anomalous co-deposition of Zn–Fe group metal alloys.[29] The progressive increase in the thickness of the coatings with CD is reasoned by Faraday's law. Furthermore, the increase in hardness at high CD is attributed to the high weight percentage of noble metal (Co) in the deposit. At 3·0 A dm^{-2}, the coating is found to be less corrosive ($19{\cdot}51 \times 10^{-2}$ mm/year) compared to coatings at other current densities. Hence, the same has been taken as optimal CD for the deposition of monolithic Zn–Co alloy.

Optimisation of CCCDs

In the case of CMMA alloys of Zn–Fe group metals, even a small change in the concentration of the latter may result in a significant change in properties due to the change in phase structure. The electrodeposition of CMMA Zn–Ni coating from a single acidic bath by potentiostatic method was reported by Ganeshan *et al.*[16] It was found that the Ni content varied as a function of thickness by applying a varying potential sequence. It was concluded that at higher potentials, the γ phase corresponding to (600) planes is preferentially deposited, while lower potentials lead to the deposition of other crystal planes of γ phases (222), (330) and (444). With this incentive, it was attempted to bring modulation in CMMA Zn–Co coatings using different current pulses. Precise control of CCCDs allowed the production of layers of Zn–Co with different compositions and, consequently, different properties. The most important requirement for the CMMA materials to exhibit

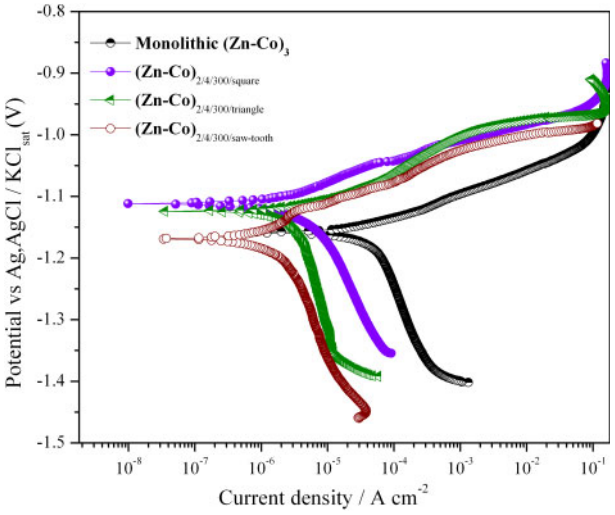

2 Potentiodynamic polarisation behaviours of $(Zn–Co)_3$, $(Zn–Co)_{2/4/300/square}$, $(Zn–Co)_{2/4/300/triangular}$ and $(Zn–Co)_{2/4/300/sawtooth}$ coating systems of same thickness

Table 2 Corrosion rates of monolithic $(Zn–Co)_3$ and CMMA coatings of different configurations developed using square, triangular and sawtooth current pulses at CCCDs of 2·0 and 4·0 A dm^{-2}

Coating configuration	$-E_{corr}$(Ag,AgCl/KCl_{sat})/V	i_{corr}/μA cm^{-2}	Corrosion rate CR/$\times 10^{-2}$ mm/year
$(Zn–Co)_3$	1·158	13·15	19·51
CMMA coatings using square pulses			
$(Zn–Co)_{2/4/10}$	1·06	9·32	13·87
$(Zn–Co)_{2/4/20}$	1·07	8·02	11·91
$(Zn–Co)_{2/4/60}$	1·09	2·81	4·18
$(Zn–Co)_{2/4/120}$	1·09	0·67	1·00
$(Zn–Co)_{2/4/300}$	1·11	0·124	0·18
$(Zn–Co)_{2/4/600}$	1·11	9·03	13·4
$(Zn–Co)_{2/4/900}$	1·09	12·09	17·94
CMMA coatings using triangular pulses			
$(Zn–Co)_{2/4/10}$	1·12	8·30	12·31
$(Zn–Co)_{2/4/20}$	1·14	5·04	7·48
$(Zn–Co)_{2/4/60}$	1·13	1·31	1·95
$(Zn–Co)_{2/4/120}$	1·11	0·59	0·88
$(Zn–Co)_{2/4/300}$	1·12	0·174	0·24
$(Zn–Co)_{2/4/600}$	1·13	7·64	11·34
$(Zn–Co)_{2/4/900}$	0·99	10·16	15·07
CMMA coatings using sawtooth pulses			
$(Zn–Co)_{2/4/10}$	1·17	9·02	13·39
$(Zn–Co)_{2/4/20}$	1·14	7·35	10·91
$(Zn–Co)_{2/4/60}$	1·17	4·27	6·34
$(Zn–Co)_{2/4/120}$	1·15	1·38	2·05
$(Zn–Co)_{2/4/300}$	1·16	0·158	0·22
$(Zn–Co)_{2/4/600}$	1·17	8·56	12·70
$(Zn–Co)_{2/4/900}$	1·20	14·0	20·87

improved property is a clear demarcation between layers without interlayer diffusion. To achieve this, the CCCDs should be properly selected before to go for a high degree of layering. Hence, a few sets of CCCDs have been selected arbitrarily (based on the nature of the monolithic alloy coating), and CMMA coatings have been developed. By fixing some number of layers (say 10 layers), the coatings with different configurations were developed, and their corrosion rates were measured. This procedure allowed the selection of proper CCCDs at which the coating is most resistant to corrosion. Thus, among the different sets of CCCDs tried, the results pertaining to 2·0 and 4·0 A dm^{-2} CCCDs were more encouraging. Hence, the same has been taken as optimal CCCDs for the development of CMMA coatings. Furthermore, the weight percentage of Co in the deposit at 2·0 and 4·0 A dm^{-2} was found to be 1·77 and 2·10 respectively.

Optimisation of number of layers

The properties of CMMA coatings, including their corrosion resistance, may often be improved by increasing the total number of layers (usually, up to an optimal number), as long as interlayer diffusions are not there. Therefore, at the optimal combination of current densities identified before (2·0/4·0 A dm^{-2}), CMMA coatings with 10, 20, 60, 120, 300, 600 and 900 layers were produced. It was observed that the corrosion rates are decreased substantially as the number of layers was increased only up to 300 layers and then decreased in all three types of current pulses. The least corrosion rates of $0{\cdot}18\times10^{-2}$, $0{\cdot}24\times10^{-2}$ and $0{\cdot}22\times10^{-2}$ mm/year were observed for square, triangular and sawtooth current pulses, which are represented as $(Zn–Co)_{2/4/300/square}$, $(Zn–Co)_{2/4/300/triangular}$ and $(Zn–Co)_{2/4/300/sawtooth}$ respectively, as shown in Table 2. It was found that CMMA $(Zn–Co)_{2/4/300/square}$ is the optimum configuration of the coating system for peak corrosion resistance. Under optimal condition, the thickness of each layer in the CMMA $(Zn–Co)_{2/4/300}$ coating system was calculated from the total thickness ($\sim$20 μm for bath under the set condition) and the number of layers allowed to form (300). It was found that the thickness of each layer is $\sim$66 nm.

The increase in corrosion rate at a high degree of layering (like 600 and 900 layers) in all three types of current pulses is attributed to the less relaxation time for redistribution of solutes in the diffusion layer during plating.[27] As the number of layers increased, the time for the deposition of each layer, say $(Zn–Co)_1$, is small (as the total time for deposition remains same). At a high degree of layering, there is no sufficient time for the metal ions to relax (against diffusion under given CD) and deposit on the cathode, with modulation in composition. As a result, at a high degree of layering, modulation in composition is not likely to take place. In other words, the CMMA deposit is tending towards monolithic, showing less corrosion resistance.

Corrosion study

Potentiodynamic polarisation study

To identify the significance of current pulses on the corrosion behaviour, the depositions were carried out using different current pulses, and their corrosion resistances were measured and compared with that of monolithic Zn–Co alloy, which was represented as $(Zn–Co)_3$. It may be observed that the CMMA coating systems are more corrosion resistant than monolithic $(Zn–Co)_3$ alloy coatings, as shown in Table 2. The polarisation curves of the $(Zn–Co)_3$, $(Zn–Co)_{2/4/300/square}$, $(Zn–Co)_{2/4/300/triangular}$ and $(Zn–Co)_{2/4/300/sawtooth}$ coating systems shown in Fig. 2 demonstrate a substantial decrease in corrosion rate compared to monolithic alloy of the same thickness.

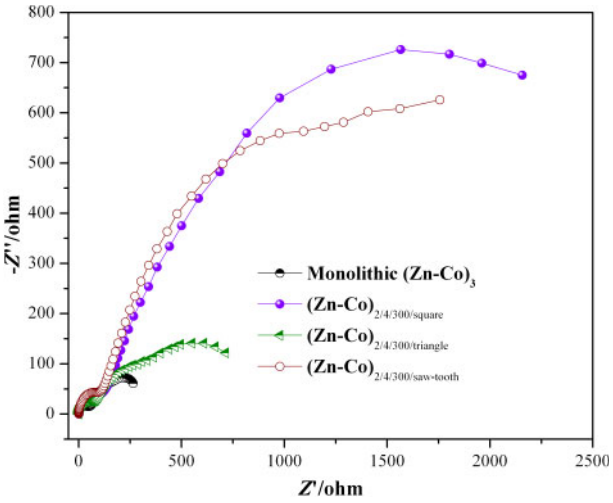

3 Electrochemical impedance response of monolithic and CMMA $(Zn–Co)_{2/4/300}$ coatings measured at frequency range of 100 kHz–10 mHz with perturbing voltage of 10 mV

Electrochemical impedance study

The EIS technique is one of the powerful tools for studying the electrochemical behaviour of the materials. In this technique, the impedance behaviour is being studied using an ac signal of small amplitude.[30–32] The impedance response of CMMA coatings developed using different types of power patterns is shown in Fig. 3. Approximately semicircle capacitive loops with increasing radii demonstrated that the CMMA coatings display better corrosion resistance than monolithic $(Zn–Co)_3$ alloy. The distortion of the capacitance loops may be due to the electrode surface roughness or distribution/accumulation of the charge carriers.

Dielectric barrier of coatings

The EIS data points can also be used to study the dielectric properties of materials, and the technique is called dielectric spectroscopy. It is based on the interaction of an external field with the electric dipole moment of the sample, which is often expressed by permittivity. This technique measures the relative dielectric constant of a system over a range of frequencies, and the frequency response of the system, including the energy storage, and the dissipation properties can be identified.

In the presence of a material having dielectric constant ε_M, the surface charge density on the plates of a capacitor may be represented by[30]

$$\sigma = \varepsilon_M E + P \quad (1)$$

where σ is the surface charge density or quantity of charge per unit area of capacitor plate (C m^{-2}) and is proportional to the electric field E and polarisation P or the increase in the electric charge density above that for a vacuum because of the presence of the dielectric. For

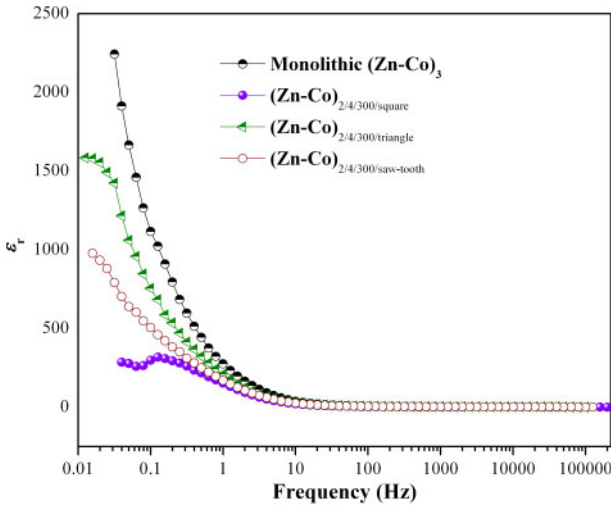

4 Variation in ε_r with frequency for different coating systems: $(Zn–Co)_3$, $(Zn–Co)_{2/4/300/square}$, $(Zn–Co)_{2/4/300/triangular}$ and $(Zn–Co)_{2/4/300/sawtooth}$

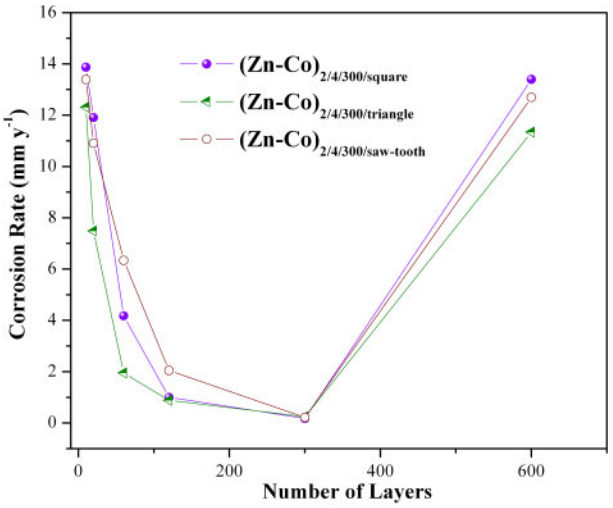

5 Variation in corrosion rates with number of layers in CMMA coatings developed using square, triangular and sawtooth current pulses

many dielectric materials, P is proportional to E through the relationship

$$P=\varepsilon_0(\varepsilon_r-1)E \quad (2)$$

where ε_0 is the dielectric constant of vacuum, and ε_r is the relative dielectric constant of the medium.

The improved corrosion resistance of the multilayer coating can also be explained in terms of the changed dielectric property of the material due to coatings. The equation for the dielectric constant ε_r is written as[33,34]

$$\varepsilon_r=\frac{Z_I}{\omega C_0(Z_R^2+Z_I^2)} \quad (3)$$

here, $C_0=\varepsilon_0 A/t$, and ε_0 is the permittivity of free space, A is the electrolyte–electrode contact area and t is the thickness of the dielectric medium, and $\omega=2\pi f$, with f being the frequency in hertz. Z_R and Z_I are the real and imaginary parts of the complex impedance spectra $Z^*=Z_R+jZ_I$.

The variations of ε_r with frequency from 10 mHz to 100 kHz for different coatings, namely, $(Zn–Co)_3$, $(Zn–Co)_{2/4/300/square}$, $(Zn–Co)_{2/4/300/triangular}$ and $(Zn–Co)_{2/4/300/sawtooth}$, are shown Fig. 4. It may be observed that ε_r of all coatings is dependent on the frequency at the lower limit and almost independent of it at the higher limit. It is due to the fact that, at high frequencies, there is no charging of the capacitor, and the capacitance is effectively like that of an open circuit (vacuum). Hence, ε_r is almost the same, irrespective of the type of current pulse used. At low frequency, the capacitor will be charged, and the capacitance is effectively like that of a closed circuit.[35,36] Under this condition, the capacitance of the electrical double layer depends on the value of ε_r. It may be observed that the value of ε_r for CMMA $(Zn–Co)_{2/4/300/square}$ is small compared to that of other coating systems, as shown in Fig. 4. The high ε_r of $(Zn–Co)_3$ indicates the high space charge density of the monolithic alloy, as required by equation (2). Hence, more space charge carriers have to flow from the positive to the negative plate to re-establish the voltage. However, in the case of CMMA $(Zn–Co)_{2/4/300/square}$, the space charge density is very small compared to monolithic and also other coating systems. Therefore, it may be inferred that the better corrosion resistance of CMMA $(Zn–Co)_{2/4/300/square}$ coatings is due to the impeded movement of charge carriers at the interface, which is caused by layering using square pulses. This may be due to the sharp change in composition in the successive layers.

Comparison of corrosion behaviours of monolithic and CMMA coatings

A comparative account of corrosion data of CMMA coatings developed using square, triangular and sawtooth pulses, in comparison with that of monolithic Zn–Co alloys of the same thickness (under optimal condition) is shown in Table 3. It was found that the corrosion protection of the $(Zn–Co)_{2/4/300/square}$ coating system is $\sim$100 times better ($0{\cdot}18\times10^{-2}$ mm/year) than that of monolithic $(Zn–Co)_3$ alloy ($19{\cdot}51\times10^{-2}$ mm/year) deposited for the same length of time. Furthermore, the coating systems having the configuration of $(Zn–Co)_{2/4/300/triangular}$ and $(Zn–Co)_{2/4/300/sawtooth}$ exhibit $\sim$80 and 90 times better corrosion resistance compared to $(Zn–Co)_3$ respectively. The observed high corrosion resistance of the coatings produced using pulsed current is attributed to the additional interfaces in the coating lattice caused by either gradual or sudden change in CD. Furthermore, among the different current pulses used,

Table 3 Comparison of corrosion rates of $(Zn–Co)_3$ (monolithic) and CMMA coating systems of same thickness

Coating configuration	$-E_{corr}$(Ag,AgCl/KCl$_{sat}$)/V	i_{corr}/μA cm^{-2}	CR/$\times10^{-2}$ mm/year
$(Zn–Co)_3$ (monolithic)	1·15	13·15	19·51
$(Zn–Co)_{2/4/300/square}$	1·11	0·124	0·18
$(Zn–Co)_{2/4/300/triangular}$	1·12	0·178	0·24
$(Zn–Co)_{2/4/300/sawtooth}$	1·16	0·158	0·22

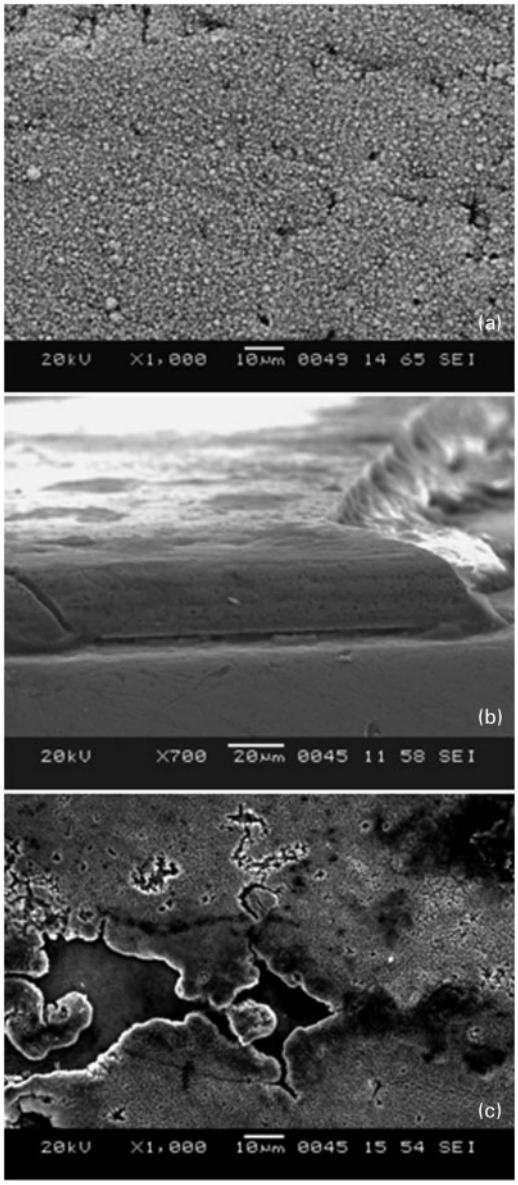

6 Images (SEM) of monolithic Zn–Co coatings under optimal condition: *a* surface morphology of $(Zn–Co)_3$ coating; *b* cross-sectional view; *c* surface after corrosion test under optimal condition

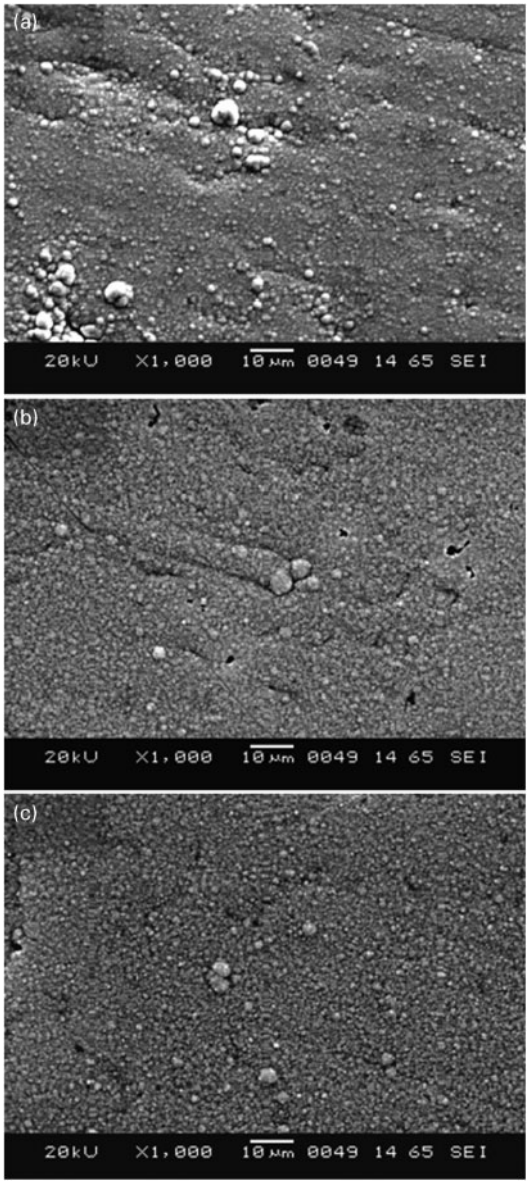

7 Surface morphology of CMMA coating systems under optimal condition: *a* $(Zn–Co)_{2/4/20/square}$; *b* $(Zn–Co)_{2/4/20/triangular}$; *c* $(Zn–Co)_{2/4/20/sawtooth}$

the coatings developed using square current pulses exhibit higher corrosion resistance due to the sharp change in the CD. Furthermore, the relatively less corrosion resistances of $(Zn–Co)_{2/4/300/triangular}$ and $(Zn–Co)_{2/4/300/sawtooth}$ coatings are due to the gradual change in CD during plating.

The variation in corrosion rates of CMMA coatings with number of layers is shown in Fig. 5. It may be observed that in all CMMA coatings, the corrosion rate decreases sharply with the increase in number of layers only at a lower degree of layering and then takes a saturation value. It may be noted that it is more pronounced in the case of coatings developed using square pulses than those obtained from triangular and sawtooth pulses. It may be due to the fact that square pulses allowing a sharp modulation in composition. Furthermore, the increase in corrosion rate at a higher degree of layering, like 600 layers (in all three types of current pulses), is due to the less relaxation time for the redistribution of metal ions (Zn^{2+} and Co^{2+} ions) in the diffusion layer, as discussed in the section on 'Optimisation of number of layers'.

Scanning electron microscopy study

The SEM images of the monolithic coating were found to be uniform, as shown in Fig. 6*a*. The formation of a monolithic alloy having no modulation in composition was confirmed from its cross-sectional view shown in Fig. 6*b*. To understand the corrosion mechanism, the coatings were subjected to anodic polarisation at ± 250 mV versus open circuit potential in 5%NaCl solution. The corroded specimens were washed with distilled water and examined under SEM. The micrograph of $(Zn–Co)_3$, displaying the surface covered with corrosion product, is shown in Fig. 6*c*. A part of the corrosion products must have been detached from the coating surface during the corrosion, and it appears as pits. This indicates that the corrosion followed the selective dissolution of less noble metal in the deposit.

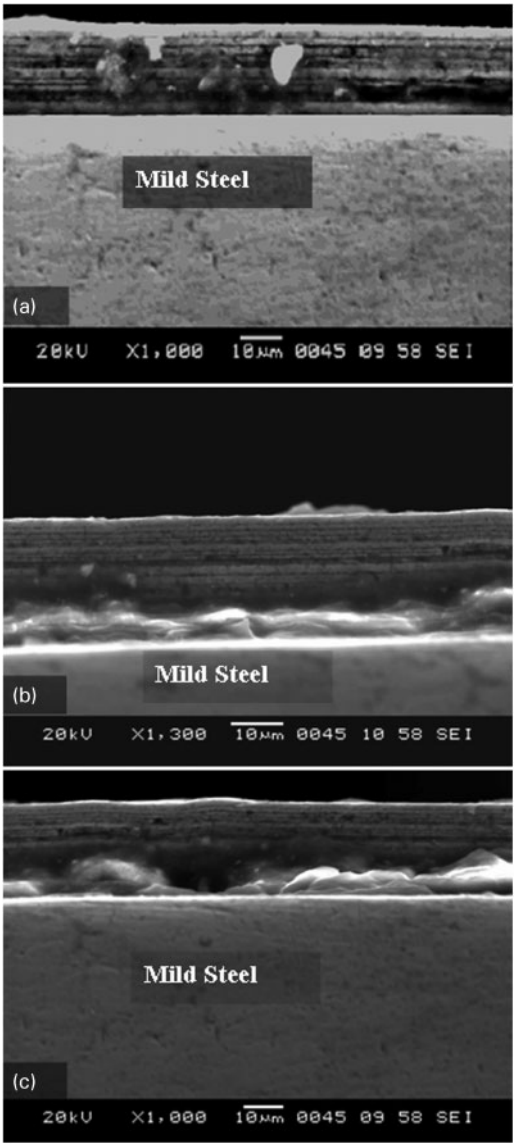

8 Cross-sectional view of CMMA coatings under optimal condition: *a* $(Zn–Co)_{2/4/20/square}$; *b* $(Zn–Co)_{2/4/20/triangular}$; *c* $(Zn–Co)_{2/4/20/sawtooth}$

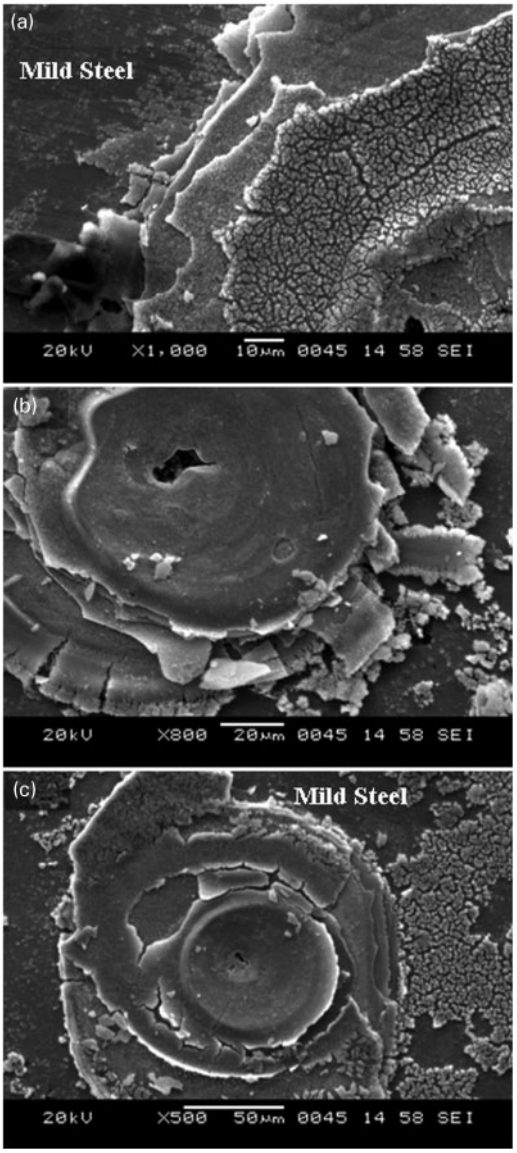

9 Cross-sectional view of CMMA coating systems after corrosion test under optimal condition: *a* $(Zn–Co)_{2/4/6/square}$; *b* $(Zn–Co)_{2/4/6/triangular}$; *c* $(Zn–Co)_{2/4/6/sawtooth}$

The surface morphologies of $(Zn–Co)_{2/4/20/square}$, $(Zn–Co)_{2/4/20/triangular}$ and $(Zn–Co)_{2/4/20/sawtooth}$ coatings were found to be relatively smooth, uniform and crack free, as shown in Fig. 7 respectively. The formation of successive layers with distinct properties was confirmed by cross-sectional view of CMMA coatings $(Zn–Co)_{2/4/20/square}$, $(Zn–Co)_{2/4/20/triangular}$ and $(Zn–Co)_{2/4/20/sawtooth}$, as shown in Fig. 8 respectively. The poor contrast in the cross-sectional view of CMMA coatings may be due to the marginal difference in chemical composition of the alloys in alternate layers. The white region observed at the interface of the metal and multilayer coating, observed in Fig. 8*b* and *c* is attributed to the scattering of electrons due to the alumina based suspension used while polishing the SEM specimen.

The SEM images of corroded CMMA coatings having six layers (for better distinction), which are represented as $(Zn–Co)_{2/4/6/square}$, $(Zn–Co)_{2/4/6/triangular}$ and $(Zn–Co)_{2/4/6/sawtooth}$, are shown in Fig. 9. Inspection of the microscopic appearance of the surface allows understanding the mechanism of corrosion, with possible reasons for improved corrosion resistance. The high corrosion prevention is due to the fact that one layer of alloy having one type of failure (like pores, crevices or columnar structure), due to deposition at one CD, will be covered successively by the another layer of alloy having another type of failure (due to deposition at some other CD). Thus, the coatings possess alternate layers having different degrees of failures, and thus, the corrosion agent path is longer or blocked.[12] That is why with multilayer coating, the corrosive agent needs more time to penetrate through coating defects into the substrate material than in the case of monolayer coating. In other words, the corrosive agent path is extended or blocked. The Zn–Co alloy layer, with less weight percentage of Co beneath the high weight percentage of Co top layer, dissolves through the pores and microcracks existing in the CMMA coatings existing during corrosion.[23] As a whole, the protection efficacy of CMMA Zn–Co coatings may be explained by the barrier effect of the Zn–Co layer, with high weight

percentage of Co (2·10), and the sacrificial effect of Zn–Co layer, with less weight percentage of Co (1·77).

Conclusion

1. The CMMA coatings of Zn–Co have been developed through SBT using different types of cyclic current pulses, namely, square, triangular and sawtooth, and their corrosion behaviours were studied.

2. The corrosion resistance of CMMA coatings increased with the number of layers up to 300 and then decreased in all types of current pulses.

3. Under optimal conditions, the coatings developed using square, triangular and sawtooth current pulses were found to be respectively ~100, 80 and 90 times more corrosion resistant than monolithic alloy of the same thickness. The order of corrosion resistance is $(Zn–Co)_{2/4/300/square} > (Zn–Co)_{2/4/300/sawtooth} > (Zn–Co)_{2/4/300/triangular}$.

Acknowledgements

The authors acknowledge the financial assistance provided by the Department of Science Technology (DST), New Delhi, India (grant no. SR/S2/CMP/0059/2006 dated 22 October 2007).

References

1. K. S. Ranga Krishnan, K. Srinivasan and S. Mohan: *Trans. Inst. Met. Finish.*, 2002, **80**, 46–48.
2. M. R. Kalantary, G. D. Wilcox and D. R. Gabe: *Electrochim. Acta*, 1995, **40**, 1609–1616.
3. A. Haseeb, J. Celis and J. Roos: *Trans. Inst. Met. Finish.*, 1992, **70**, 123–128.
4. A. Haseeb, J. Celis and J. Roos: *J. Electrochem. Soc.*, 1994, **141**, 230–237.
5. D. R. Gabe and W. Green: *Surf. Coat. Technol.*, 1998, **105**, 195–201.
6. D. Pilone and U. Bernabai: *Surf. Eng.*, 2008, **24**, 193–197.
7. P. E. Hovsepian, A. P. Ehiasarian and I. Petrov: *Surf. Eng.*, 2010, **26**, 610–614.
8. E. Arslan: *Surf. Eng.*, 2010, **26**, 615–619.
9. L. E. Gil, S. Liscano, P. Goudeau, E. Le Bourhis, E. S. Puchi-Cabrera and M. H. Staia: *Surf. Eng.*, 2010, **26**, 562–566.
10. U. Figueroa, O. Salas and J. Oseguera: *Surf. Eng.*, 2006, **22**, 109–120.
11. Y. N. Kok, J. G. Wen, I. Petrov and P. Eh. Hovsepian: *Surf. Eng.*, 2006, **22**, 92–98.
12. L. A. Dobrzanski, K. Lukaszkowicz, D. Pakula and J. Mikula: *Arch. Mater. Sci. Eng.*, 2007, **28**, 12–18.
13. G. D. Wilcox and D. R. Gabe: *Corros. Sci.*, 1993, **35**, 1251–1258.
14. I. Ivanov, T. Valkova and I. Kirilova: *J. Appl. Electrochem.*, 2002, **32**, 85–89.
15. U. Cohen, F. B. Koch and R. Sard: *J. Electrochem. Soc.*, 1983, **130**, 1987–1995.
16. P. Ganeshan, S. P. Kumaraguru and B. N. Popov; *Surf. Coat. Technol.*, 2007, **201**, 7896–7904.
17. M. E. Bahrololoom, D. R. Gabe and G. D. Wilcox: *J. Electrochem. Soc.*, 2003, **150**, C144–C151.
18. I. Ivanov and I. Kirilova: *J. Appl. Electrochem.*, 2003, **33**, 239–244.
19. H. Nikdehghan, A. Amadeh and A. Honarbakhsh-Raouf: *Surf. Eng.*, 2008, **24**, 287–294.
20. D. Chaliampalias, N. Pistofidis and G. Vourlias: *Surf. Eng.*, 2008, **24**, 264–267.
21. M. R. Kalantary, G. D. Wilcox and D. R. Gabe: *Br. Corros. J.*, 1998, **33**, 197–201.
22. G. Chawa, G. D. Wilcox and D. R. Gabe: *Trans. Inst. Met. Finish.*, 1998, **76**, 117–120.
23. J.-Y. Fei, G.-Z. Liang, W.-L. Xin and W.-K. Wang: *J. Iron. Steel Res. Int.*, 2006, **13**, 61–67.
24. J.-Y. Fei, G.-Z. Liang, W.-L. Xin and J. Liu: *J. Wuhan Univ. Technol.*, 2006, **21**, 40–44.
25. G. D. Wilcox: *J. Corros. Sci. Eng.*, 2004, **6**, 52.
26. V. Thangaraj, N. Eliaz and A. Chitharanjan Hegde: *J. Appl. Electrochem.*, 2009, **39**, 339–345.
27. N. Kanani: 'Electroplating: basic principles, processes and practice'; 2006, Berlin, Elsevier Ltd.
28. A. I. Vogel: 'Quantitative inorganic analysis'; 1951, London, Longmans Green and Co.
29. A. Brenner: 'Electrodeposition of alloys', Vol. 2, 589; 1963, New York, Academic Press.
30. P. J. Gellings and H. J. M. Bouwmeester: 'Handbook of solid state electrochemistry'; 1997, Boca Raton, FL, CRC Press..
31. E. Akbarinezhad and H. R. Faridi: *Surf. Eng.*, 2008, **24**, 280–286.
32. S. Sarac, B. Schulz, A. Gencturk and H. D. Gilsing: *Surf. Eng.*, 2008, **24**, 358–365.
33. A. S. Bhatt, D. Krishna Bhat and M. S. Santosh: *Physica B*, 2010, **405B**, 2078–2082.
34. C. G. Koops: *Phys. Rev.*, 1951, **83**, 121–124.
35. X. Yuan, C. Song, H. Wang and J. Zhang: 'Electrochemical impedance spectroscopy in PEM fuel cells – fundamentals and applications'; 2010, London, Springer Publications.
36. D. Ravinder and K. Latha: *Mater. Lett.*, 1999, **41**, 247–253.